

Comparative Study on Ability of Some Magnetic Nanocompounds of Fe₃O₄, Fe₃O₄/Polystyrene and Fe₃O₄/Polyaniline to Remove of Methyl Orange from Aqueous Solutions

Robab Mohammadi*, Bakhshali Massoumi, Amin Mashayekhi

Department of Chemistry, Payame Noor University, PO box 19395-3697, Tehran, Iran

Received: 6 August 2023

Accepted: 10 September 2023

DOI: [10.30473/ijac.2023.68776.1272](https://doi.org/10.30473/ijac.2023.68776.1272)

Abstract

In this research, Fe₃O₄, Fe₃O₄/polystyrene and Fe₃O₄/polyaniline nanocompounds were prepared and compared on the removal of methyl orange from aqueous solutions. The chemical structures of the synthesized compounds were studied using FT-IR. The crystalline phase of Fe₃O₄, Fe₃O₄/polystyrene and Fe₃O₄/polyaniline nanocompounds was characterized by XRD. SEM was used for detecting morphology of the synthesized samples. The magnetic property of the prepared samples was successfully checked. The prepared nanocompounds were used to remove methyl orange as an anionic dye from aqueous solutions. Based on results, Fe₃O₄/polyaniline nanocomposite showed higher efficiency in the removal of methyl orange, which is partly due to the oppositely charged methyl orange and Fe₃O₄/polyaniline. Effective variables on the removal of methyl orange such as adsorbent dosage, pH, and contact time were studied and optimized. At the optimum situations the pH, catalyst dosage, and time were 3-4, 450 mg L⁻¹, and 50 min, respectively. For detecting the type of adsorption isotherm, Langmuir, Freundlich, and Dubinin Radushkevich adsorption isotherms were studied. According to Langmuir model, Fe₃O₄/polyaniline magnetic adsorbent showed the highest methyl orange adsorption capacity of 48.76 mg g⁻¹. Kinetic studies proved that methyl orange adsorption was explained more accurately via pseudo-second order model compared to the pseudo-first order model. Under controlled reaction conditions, Gibbs free energy (ΔG°) varied from -1.41 to -1.69 kJ mol⁻¹, besides, the resulting ΔH° and ΔS° quantities were obtained 4.07 kJ mol⁻¹ and 0.018 kJ mol⁻¹K⁻¹, respectively. Therefore, it can be considered that the adsorption of methyl orange onto the Fe₃O₄/polyaniline magnetic adsorbent is a spontaneous and endothermic procedure.

Keywords

Fe₃O₄/polystyrene; Fe₃O₄/polyaniline; Removal of methyl orange; Adsorption capacity; Kinetic studies.

1. INTRODUCTION

Water pollution is a major problem because of its harmful and dangerous impact on ecosystems and human health. Dye effluent, especially, has become an important source of water pollution and is very hard to decompose because of its high toxicity and carcinogenicity [1,2]. It is therefore greatly desirable to make constructive and useful methods for removing the dye pollutants from wastewater. Different methods are available for the removal of pollutants, including chemical composition, coagulation/flocculation, membrane procedures, ion exchange, photo oxidation, reverse osmosis and adsorption process [3].

Adsorption is a procedure by which compounds in a solution are adsorbed onto an adsorbing material. The adsorption procedure has a high efficiency compared to other treatment procedures and is able to remove higher concentrations with lower cost [4]. Different adsorbents such as carbon nanotubes, Magnetic core-zeolitic shell, multiwall carbon nanotubes (MWCNTs), nanoparticles and nanocomposites, activated carbon, graphene

nanostructures and conductive electroactive polymers such as polypyrrole and polyaniline were applied to remove different pollutants from water and wastewater [5]. Similarly, various metal oxides such as ZnO, TiO₂, MoO₃, WO₃, Fe₃O₄, ZrO₂, etc were employed for the adsorption of organic dyes from wastewater [4-6]. The most important criterion in the selection of adsorbents to be applied in the adsorption procedure is that it is easy to find, cheap, and reusable. Despite these materials, from the last few years, a lot of focus has been done on polymer-based adsorbent since the polymer exhibited large surface area, high porosity, and selectivity for the adsorption of the dyes[7]. Among the class of polymer, polyaniline has attracted special attention because of its high adsorption capacity, simple synthesis, environmental stability and simple doping/dedoping chemistry. The presence of amine and imine groups in polyaniline is the active species for the dye adsorption. Despite this property, polyaniline exhibits good mechanical stability, a highly porous structure, and large surface area with low cost, and the easy availability

* Corresponding author:

R. Mohammadi; E mail; rb_mohammadi@pnu.ac.ir; mohammadi_rb@yahoo.com

of aniline (monomer of polyaniline)[8]. Ayad *et al.* studied the adsorption of methylene blue using polyaniline nanotube for the effective removal of dye because of the chemical interaction of polyaniline with the dye molecule [9]. Similarly, Sharma *et al.* have fabricated crosslinked nanoporous polyaniline with a large surface area and employed for the removal of both cationic and anionic dye [10]. Although polyaniline is used on a large scale for adsorption of dyes, there is some obstacle for using it. The poor interaction with dye molecule, difficult separation, and regeneration of adsorbent led to the limited use of it. The increasing research in this field has resolved the problem by producing nanocomposite of the polymer-based compound with metal oxides which leads to the easy separation of the adsorbent material[11]. When combined with a magnetic particles, the composite can have a magnetic property. As a result, the composite can form a constant suspension in an aqueous solution and is immediately separated from the external environment. Therefore, the obtained composite may have great potential for catalysis and environmental remediation [12]. Magnetic separation is a kind of efficient, rapid and inexpensive technique to separate adsorbents from solution. Thus far, magnetic polymer-based adsorbents have been prepared using different approaches for removal of pollutants. Therefore, generation of magnetic nanocomposite without obvious toxicity is an important task for many applications. Moreover, between different types of magnetic materials, iron oxide (Fe_3O_4) is the best choices because of its special magnetic properties, low toxicity, chemical stability, low cost and simplicity of separation from aqueous solution compared to other adsorbents [13]. Several magnetic nanocomposites, including Fe_2O_3 /graphene/ CuO , $\text{rGO-Fe}_3\text{O}_4$, Fe_3O_4 / ZnO , Fe_3O_4 /alginate, Fe_3O_4 /polystyrene, Fe_3O_4 /polyaniline and various other NPs, have recently been used as catalytic materials to achieve excellent degradation efficiency of organic dyes [14]. For instance, Monsef *et al.* [15] have explored $\text{g-C}_3\text{N}_4/\text{Fe}_2\text{O}_3/\text{EuVO}_4$ ternary nanocomposite for photocatalyst and hydrogen storage application. They have achieved 80.06% removal of Rhodamine B using visible sources. Abdalkareem Jasim *et al.* [16] reported photocatalytic degradation of rhodamine B (RhB) and methylene blue (MB) dyes under visible light irradiation using $\alpha\text{-Fe}_2\text{O}_3$ nanoparticles.

The polymer-iron oxide composite, which shows special magnetic and supercapacitance properties, has attracted much attention for environmental application, including for use in treatment of water, as a catalyst and in magnetic separations. For example, Tran *et al.* prepared a magnetic

Polyaniline/ Fe_3O_4 -Hydrotalcite for efficient removal of methyl orange (MO) from wastewater [17]. Mohammadi *et al.* prepared Fe_3O_4 /polystyrene-alginate nanocomposite with high adsorption capacity for removal of malachite green as a cationic dye from aqueous solutions [18]. On the other hand, polymers are frequently applied for surface modification of Fe_3O_4 nanoparticles because of several advantages which make them suitable in the catalytic applications. For an instance, polymer coatings can be generated to verify the surface properties of superparamagnetic nanoparticles, to enhance the compatibility between nanoparticles and aqueous medium, to prevent particle surface from oxidation, to decline toxicity and to facilitate storage or transport, to physically adsorb compounds [19].

The aim of the present research was to prepare Fe_3O_4 , Fe_3O_4 /polystyrene and Fe_3O_4 /polyaniline magnetic nanocompounds and compare their adsorption capacity for the removal of methyl orange as an anionic dye from aqueous solutions. To the best of our knowledge, there is no report on the comparison of adsorption capacity between Fe_3O_4 /polystyrene and Fe_3O_4 /polyaniline nanocomposites. Also, various adsorption parameters such as contact time, adsorbent dosage, and pH of the solution were investigated. Moreover, kinetics (pseudo-first and pseudo-second order), equilibrium isotherms (Langmuir, Freundlich, and Dubinin Radushkevich models), and thermodynamic studies were applied in this work.

2. EXPERIMENTAL

2.1. Chemicals

Iron (III) chloride hexahydrate ($\text{FeCl}_3 \cdot 6\text{H}_2\text{O}$), Iron (II) chloride tetrahydrate ($\text{FeCl}_2 \cdot 4\text{H}_2\text{O}$), cetyl trimethyl ammonium bromide (CTAB), sulfuric acid, Aniline, hydrochloric acid, and sodium hydroxide are of analytical grade and are obtained from Merck, Germany. Polystyrene (PS, M_w 35×10^3) was obtained from Sigma Aldrich. Methyl orange was purchased from Alvan sabet Co., Iran and used without further purification.

2.1.1. Preparation of Fe_3O_4 nanoparticles

Fe_3O_4 nanoparticles were prepared through chemical co precipitation method as explained by Hammouda et.al. [20]. 1.5 g $\text{FeCl}_2 \cdot 4\text{H}_2\text{O}$ and 4.7 g $\text{FeCl}_3 \cdot 6\text{H}_2\text{O}$ were dissolved in 20 mL HCl (0.4 mol L^{-1}) in a beaker which was degassed with nitrogen gas for 20 min before use. 250 mL of 1.5 mol L^{-1} NaOH solution was degassed (for 15 min) and heated up to 80°C in the reactor. Then, it was added dropwise into the above solution using a dropping funnel during 30 min under nitrogen gas protection and was stirred by a hand-made stirrer. During the

whole process, the solution temperature remained at 80 °C and nitrogen gas was used to prevent the intrusion of oxygen. Upon completion of the reaction, the resulting black iron oxide nanoparticles were collected with the help of a strong magnet and washed several times with distilled water (Millipore–Aqualix, USA) and then, the product was oven dried at 90 °C.

To find out magnetite particles (Fe₃O₄) have been generated or not via bringing the solution closer to a permanent magnet. If the black solid that settles moves closer to the source of the permanent magnet, it means that the magnetite material has generated.

2.1.2. Synthesis of Fe₃O₄ /polystyrene nanocomposite

According to our previous work, in order to prepare Fe₃O₄ /polystyrene nanocomposite, 0.1 g polystyrene (Sabic company) was dissolved in 5 ml xylene. After, 0.5 g Fe₃O₄ nanoparticles were dispersed in 5 mL xylene for 20 minutes in an ultrasonic bath and added drop wise into the above solution under continuous stirring. The final product was mechanically stirred for 2 hours. Finally, the resulted nanocomposite was washed twice with 30 mL water and dried at 50 °C [18].

2.1.3. Preparation of Fe₃O₄ /polyaniline nanocomposite

Fe₃O₄/polyaniline nanocomposite was prepared as described by Tayebi et al. [21]. One gram of KIO₃ was added to 100 mL sulfuric acid (1 mol L⁻¹) and then a uniform solution was resulted using magnetic mixer. After 10 min, 1 g Fe₃O₄ nanoparticles and 0.2 g CTAB were added to the solution and after 20 min, 1 mL fresh distilled aniline monomer was added to the stirred solution. The reaction was carried out for 5 h at room temperature. Fe₃O₄ /polyaniline nanocomposite particles were separated from the reaction media by placing a strong magnet, and rinsed several times with deionized water and acetone, and dried at 60 °C temperature in an oven for 24 h and stored in a desiccator for subsequent use.

2.2. Characterization

Fourier transform infrared spectroscopy (FTIR) analysis of nanocompounds was performed on a Nicolet 560 FTIR spectrometer. The samples were prepared by mixing with KBr and pressing into a compact pellet. The crystal structure of prepared samples was recorded using X-ray diffraction (XRD) (Siemens/D5000) with Cu K α radiation (0.15478 nm) in the 2 θ scan range of 10°–70°. The morphology and texture of prepared samples were measured via scanning electron microscope (SEM, LEO 440i, Leo Electron Microscopy, Cambridge, England). Magnetic properties of the samples were

studied by the vibrating sample magnetometer (VSM), quantum design, 14 T PPMS.

2.3. Batch experimental system

The experiments were carried out in 100 ml Erlenmeyer flasks as batch experimental reactors to investigate the influences of operational factors such as the reaction time, adsorbent dosage, and initial pH on methyl orange adsorption onto prepared materials. In each run, desired concentration of methyl orange and catalyst were fed into the quartz and allowed to establish an adsorption–desorption equilibrium for 30 min and then mixed via shaking at a temperature of 25 °C. The pH was adjusted to the desirable values with 0.1 M HCl and 0.1 M NaOH at the beginning of each test. The set of experiment was conducted at an initial pollutant concentration of 20 mg L⁻¹, adsorbent dosage of 450 mg L⁻¹ and initial pH of 7 for 50 min. Then, the experimental procedure was systematically carried out. Subsequently, a magnet was applied to collect the magnetic nanocompounds and the adsorption was monitored via UV-vis Perkin-Elmer 550 SE spectrophotometer at wavelength of 465 nm.

2.3.1. Batch adsorption experiments

The removal of methyl orange from aqueous solutions in a batch system conducted in a 250 mL container with a working volume of 100 mL. Initially, the methyl orange stock solution was synthesized at a concentration of 500 mg L⁻¹, and the required various concentrations of methyl orange were synthesized daily via dilution by distilled water. In order to optimize the adsorption procedure, a certain dosage of adsorbent (150, 300, 450 and 600 mg L⁻¹) was studied under constant pH conditions, initial pollutant concentration and ambient temperature (25 °C). After detecting the optimum adsorbent, the pH of the solution was adjusted to 3 to 11, via adding 0.1 M HNO₃ and 0.1 M NaOH. The equilibrium study was performed by sampling at 0 to 50 min intervals. To investigate isotherm studies, 4 solutions were synthesized at concentrations of 10, 20, 30 and 40 mg L⁻¹ of dye. After 50 min (equilibrium time) sampling was carried out and equilibrium concentration (C_e) was measured. The samples were tested two times to ascertain the accuracy, reliability, and reproducibility of the data obtained from experimental results. After equilibrium was reached, the concentration of methyl orange in solution was detected via spectrophotometric method at 465 nm using UV-vis Perkin-Elmer 550 SE spectrophotometer. The amount of methyl orange adsorbed onto prepared samples was estimated via Eq. (1) [22]:

$$q = \frac{(C_0 - C) V}{M} \quad (1)$$

where q , C_0 and C are the amount of adsorbed dye (mg g^{-1}), the initial concentration and the final concentration of pollutant in the solution (mg L^{-1}), respectively. In addition, V is the volume of the solution (L) and M is the weight of the catalyst (g).

3.RESULTS AND DISCUSSION

1.1. Characterization of prepared nanocomposite

1.1.1. Fourier transform infrared spectroscopy (FTIR)

The FTIR spectrum of Fe_3O_4 nanoparticles is shown in Fig. 1(a). The peak at 3440 cm^{-1} are due to O–H stretching vibration arising from hydroxyl groups from the water on nanoparticles. The absorption peaks at 2926 , 2860 , 1620 and 1355.22 cm^{-1} are due to water used as solvent. The 725 and 577 cm^{-1} absorption peaks corresponds to the Fe–O bond vibration of Fe_3O_4 nanoparticles [23][Fig 1 (a)].

The FTIR spectrum of Fe_3O_4 /polyaniline is shown in Fig. 1(b). As can be seen, polyaniline shows the presence of the characteristic absorption bands at 1591 cm^{-1} (C=C stretching vibration of the quinoid ring), 1454 cm^{-1} (stretching vibration of C=C of the benzenoid ring), 1304 cm^{-1} (C–N stretching vibration), 1125 cm^{-1} (C–H in-plane deformation), and 811 cm^{-1} (C–H out of- plane deformation). It can be seen that the characteristic peak of magnetic Fe_3O_4 appeared at 561 cm^{-1} . The adsorption peak at 3600 are due to the O–H stretching vibration [24][Fig 1 (b)].

The FTIR spectrum of Fe_3O_4 /polystyrene is shown in Fig. 1(c). The strong absorption band appeared at about 561 cm^{-1} is assigned to the vibrations of the Fe–O bond, which confirm the formation of Fe_3O_4 nanoparticles. The adsorption peaks at 1442 and 1535 cm^{-1} are due to the vibration of C=C bonds in the benzene ring. The strong peak at 639 cm^{-1} and characteristic absorbing peak at 2921 cm^{-1} are corresponding to C–H of the benzene ring. The bands in the 3340 cm^{-1} region are related to the O–H stretching vibration [25]. Based on the above observation, we can find that the Fe_3O_4 nanoparticles and polystyrene exist in the composite particles [Fig1 (c)].

1.1.2. X-ray diffraction (XRD)

The X-ray diffraction patterns of the synthesized samples are alliterated in Fig. 2. Each diffraction peak of the samples may be assigned to the cubic phase structure (JCPDS card, file no. 79-0418). The peaks at 2θ values: 29.7 , 35.5 , 43.1 , 53.1 , 57.1 , 62.2 and 74.1° could be indexed as the (220), (311), (400), (422), (511), (440) and (553) crystal planes of cubic phase Fe_3O_4 , respectively [26].

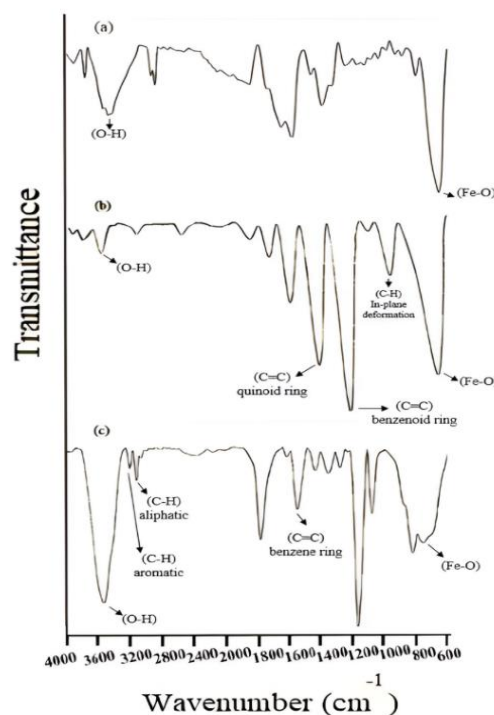


Fig. 1. FTIR spectra of (a) Fe_3O_4 , (b) Fe_3O_4 /polyaniline, and (c) Fe_3O_4 /polystyrene samples.

The sharpness of the peaks clearly indicates that the prepared particles had a highly crystalline nature. These crystalline entities demonstrate the typical pattern of Fe_3O_4 , and there was no other phase such as Fe_2O_3 or $\text{Fe}(\text{OH})_3$, which were the usual co-products in chemical reverse coprecipitation procedure. It can be clearly seen from the XRD pattern that Fe_3O_4 's characteristic diffraction peaks have been retained well in both Fe_3O_4 /polyaniline (Fig. 2b) and Fe_3O_4 /polystyrene (Fig. 2c) nanocomposites if compared with bare Fe_3O_4 nanoparticles (Fig. 3a), which indicates the deposition of polymer layer has no negative influence on the crystalline structure of nano Fe_3O_4 .

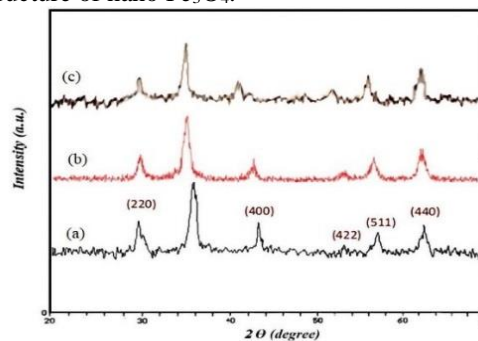


Fig. 2. XRD pattern of (a) Fe_3O_4 , (b) Fe_3O_4 /polyaniline, and (c) Fe_3O_4 /polystyrene samples.

1.1.3. SEM analysis of Fe_3O_4 /polyaniline and Fe_3O_4 /polystyrene nanocomposites

SEM image was applied to study the morphology and aggregation level of materials. Fig. 3 (a) and (b) illustrate SEM images of Fe_3O_4 /polyaniline and Fe_3O_4 /polystyrene nanocomposites respectively. The morphology of prepared nanocomposites seems to be sphere. Interestingly, the pure polymers agglomerate was not determined in SEM micrographs, which agrees with conclusions that polyaniline in Fe_3O_4 /polyaniline and polystyrene in Fe_3O_4 /polystyrene nanocomposites mainly cover the Fe_3O_4 surface. As can be observed that, SEM images show particles with good homogeneity, granular structure and slight agglomeration. Slight agglomeration is because of the formation of polyaniline or polystyrene on the surface of Fe_3O_4 nanoparticles which causes repulsion forces between nanoparticles and inhibits their agglomeration [27]. Since less particle agglomeration occurred for Fe_3O_4 /polyaniline and Fe_3O_4 /polystyrene nanocomposites, the large surface area conveys high adsorption capacities of this materials. Also, these images indicated that the average particles size of Fe_3O_4 /polyaniline and Fe_3O_4 /polystyrene nanocomposites are 10-30 and 15-50 nm respectively.

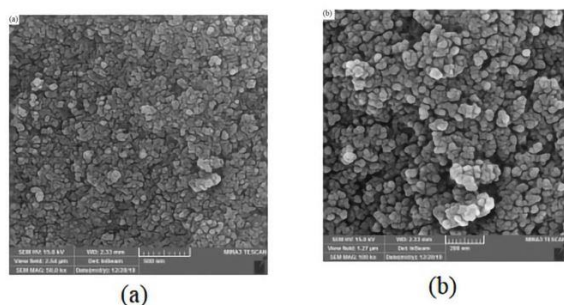


Fig. 3. SEM image of (a) Fe_3O_4 /polyaniline, and (b) Fe_3O_4 /polystyrene samples.

1.1.4. Vibrating sample magnetometer (VSM)

Fig 4 illustrated the plots of the magnetization M versus the applied magnetic field H for the prepared samples at room temperature. The hysteresis loop shows ferromagnetic behaviour. The saturation magnetization values of Fe_3O_4 , Fe_3O_4 /polystyrene and Fe_3O_4 /polyaniline samples were calculated as 62.1, 26.7 and 28.1 $emu.g^{-1}$ from the magnetization curves, respectively. It can be seen that M_S values of Fe_3O_4 /polystyrene and Fe_3O_4 /polyaniline is lower than that of pure Fe_3O_4 nanoparticles. The reduction in saturation magnetization values reflected the standard practice of normalizing the magnetization via sample volume [28]. According to the equation $M_S = \phi m_s$, M_S was attributed to the volume fraction of the particles (ϕ) and the saturation moment of a single particle (m_s) [16]. It should be noticed that

the saturation magnetization of the Fe_3O_4 /polystyrene and Fe_3O_4 /polyaniline composites depended mainly on the volume fraction of the Fe_3O_4 nanoparticles, because of the nonmagnetic polystyrene and polyaniline coating contribution to the total magnetization, resulting in the reduction of the saturation magnetization.

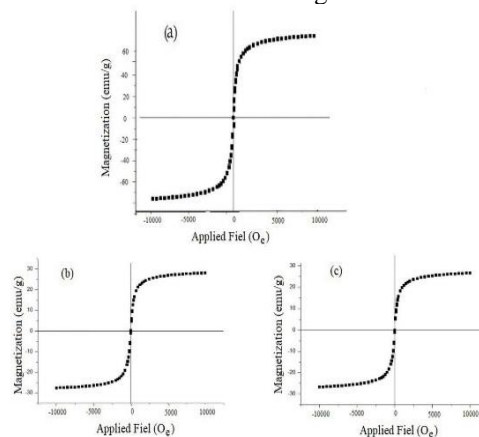


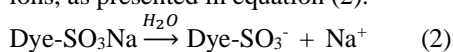
Fig. 4. Magnetization vs. applied magnetic field for (a) Fe_3O_4 , (b) Fe_3O_4 /polyaniline, and (c) Fe_3O_4 /polystyrene samples.

1.2. Adsorptive removal of methyl orange by prepared samples

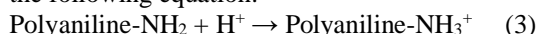
Fig 5 displays the adsorptive removal of methyl orange from aqueous solution using Fe_3O_4 , Fe_3O_4 /polystyrene and Fe_3O_4 /polyaniline samples. It could be seen that adsorptive removal of methyl orange in the presence of Fe_3O_4 /polystyrene is lower than pure Fe_3O_4 . Studying the mechanism of adsorption via the core-shell nanomaterials depends on the outer coating of these compounds. Polystyrene was investigated as an outer coating in Fe_3O_4 /polystyrene nanocomposite. Polystyrene is chemically a long chain hydrocarbon. Styrene is an aromatic molecule; aromatics are extremely stable, therefore the structure change in polystyrene is difficult. To study the adsorption procedure via nanomaterials, several parameters such as affective surface area are important [29]. The mechanism of adsorption can be explained via physical procedure involves the electrostatic interaction between adsorbate molecules and solid adsorbent, which is usually associated with low adsorption heat [30]. Ohsawa *et al.*, was investigated Zeta potential and surface charge density of polystyrene-latex and concluded that there are 2000–4000 negative charges on the its surface at $pH=7.34$. In other words, polystyrene-based adsorbents could show strong electrostatic repulsive interaction to negatively charged species.

From Fig6, adsorptive removal of methyl orange in the presence of Fe_3O_4 /polyaniline is higher than that of other samples. Via considering the adsorption of methyl orange onto the surface of

Fe₃O₄/polyaniline, various mechanisms may be involved such as ionic attraction between anionic sulfonate group(s) of dissolved methyl orange molecules and the cationic amino groups of protonated Fe₃O₄/polyaniline. The possible mechanisms of the adsorption procedure of Fe₃O₄/polyaniline and methyl orange is discussed: In aqueous solution, methyl orange can be dissolved and the sulphonate groups of methyl orange is dissociated and converted to anionic dye ions, as presented in equation (2):



In the presence of H⁺, the amino groups of polyaniline (-NH₂) can be protonated according to the following equation:



The adsorption procedure then proceeds because of the electrostatic attraction between these two counter ions. The reaction can be described by the following equation:



Adsorption process can be controlled via physical factors on most of the adsorbents such as polarity, Van der Waals forces, hydrogen bonding, dipole-dipole interaction, π - π interaction, etc. [31]. Therefore, the design of an adsorbent can be depended on the type of substance to be adsorbed or removed. Methyl orange is an anionic dye that belongs to the azo group and can be removed via an adsorbent showing strong affinity toward negatively-charged molecules. Polyaniline in its conductive emeraldine salt state possesses a large number of amine (-N<) and imine (-N=) functional groups and substantial amounts of positive charges localized over its backbone, making it an efficient candidate for the adsorption of negatively polarized materials. This electrostatic force of attraction could be the essential driving force leading to the enhanced adsorption of methyl orange. So, the presence of polyaniline in Fe₃O₄/polyaniline plays an important role in the adsorption of anionic dyes from aqueous solutions [20].

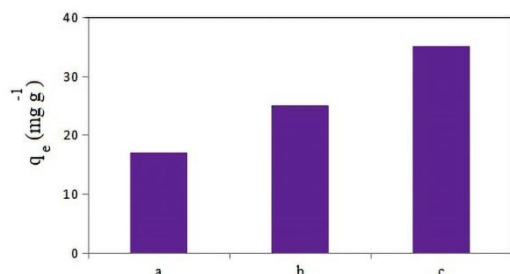


Fig. 5. Adsorptive removal of methyl orange from aqueous solution in the presence of (a) Fe₃O₄/polystyrene, (b) Fe₃O₄, and (c) Fe₃O₄/polyaniline samples.

1.2.1. Effect of contact time

Fig 6 illustrates the influence of contact time and temperature on the adsorption of methyl orange via Fe₃O₄/polyaniline nanocomposite. So, initial dye concentration of 20 mg L⁻¹, pH of 3, and Fe₃O₄/polyaniline dosage of 450 mg L⁻¹ in 100 mL were applied. The mixture was agitated in a mechanical shaker for different periods of contact time (0–80 min). The results are shown in Fig. 6. The removal of methyl orange by adsorption on Fe₃O₄/polyaniline nanocomposite was very fast during the initial contact time and then slowed down. It can be related to the sufficient exposure of adsorptive sites and the appropriate surface reactivity of the adsorbent for sequestering dye ions [32]. It can be observed from Fig. 6 that the enhancement in reaction time up to 50 min led to a little increase in adsorbed methyl orange. With passage of time, the remaining vacant surface sites are hard to be occupied due to the repulsive forces between the solute molecules on the solid phase and in the bulk liquid phase [33]. According to these findings, a contact time of 50 min was selected for more tests.

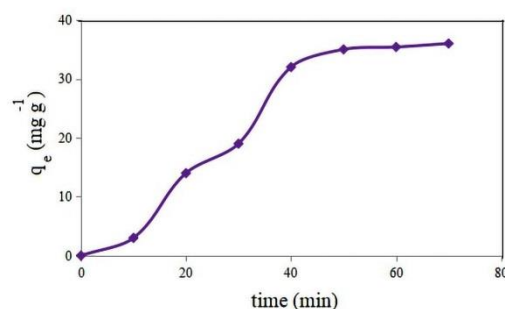


Fig. 6. Effect of contact time on the removal efficiency of methyl orange by Fe₃O₄/polyaniline nanocomposite.

1.2.2. The effect of adsorbent dosage

Different quantities of adsorbent (150 to 600 mg L⁻¹) under ambient temperature, initial dye concentration of 20 mg L⁻¹, pH 7 and contact time of 50 min were applied to investigate the adsorbent concentration. The results are illustrated in Fig. 7. By increasing the adsorbent dosage up 450 mg L⁻¹, the removal percentage of dye was increased and the equilibrium adsorption capacity was decreased (Fig 8 (a)). However, the enhancement in the adsorbent dosage to more than 450 mg L⁻¹ did not significantly affect the adsorption. After this point, because of the fact that the adsorption event was an equilibrium event, there was no significant influence of enhancing the amount of adsorbent on the pollutant removal. The enhancement in percent removal of adsorbate ions with increase in the adsorbent dosage could be related to greater availability of adsorption sites. At equilibrium, the percent removal became constant probably due to the saturation of the available adsorption sites. Equilibrium was attained at an adsorbent dosage of

450 mg L⁻¹. Another result of Fig 7 was that with the increasing dosage of the adsorbent, the adsorption capacity (q_e) declined significantly (Fig 8 (b)). As the dosage of adsorbent enhances, the percentage of pollutant removal enhances, but the adsorption capacity decreases. It is due to the existence of a large number of empty active sites in the environment compared to fixed pollutant concentration. It was believed that the adsorbate particles were massive, decline the surface area of the adsorbent, and prolong the path in the diffusion step [34].

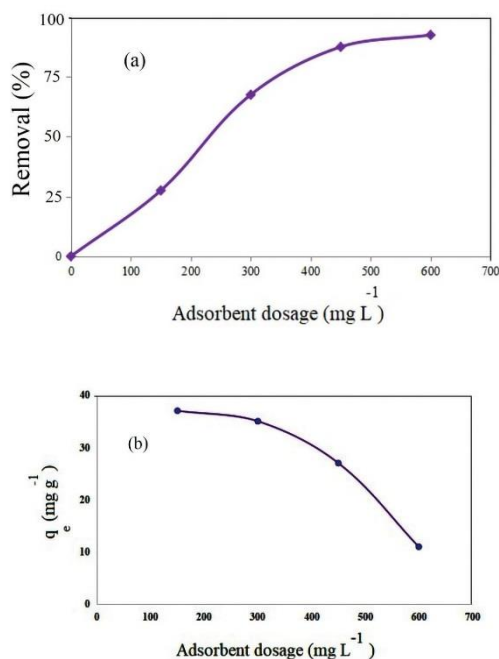


Fig. 7. Effect of adsorbent dosage on the removal efficiency of methyl orange by Fe₃O₄/polyaniline nanocomposite.

1.2.3. Effect of pH

The initial pH of the media can play an important role in the adsorption process affecting on other parameters such as surface charge of adsorbent and ionization of functional groups presenting on the active site of the adsorbent surface [24]. In order to study the influence of this factor on the adsorption, the experiments were performed at various initial pH ranging from 3 to 11. The experiment was carried out on 450 mg L⁻¹ Fe₃O₄/polyaniline nanocomposite with an initial dye concentration of 20 mg L⁻¹ at room temperature with contact time of 50 min. The results are presented in Fig. 8. Removal of methyl orange was enhanced by decreasing pH and a maximum quantity was reached at an equilibrium pH of around 3-4. In fact, at acidic pH, the amino groups of polyaniline (-NH₂) are protonated in the presence of H⁺ ions which increases the electrostatic scattering between the dye anions and

the adsorbent surface [35]. With the placement of polyaniline on the composite, more amino groups of polyaniline were available. Thus, more dye was adsorbed on the composite. At higher pH, the number of OH⁻ ions increases in the media and competes with methyl orange as an anionic dye. This can reduce the adsorption of methyl orange. On the other hand, with decreasing the pH, the competition between OH⁻ ions and anionic ions of methyl orange decreases and methyl orange mainly occupies adsorbent sites. So, experiments were performed at optimum pH of 3-4.

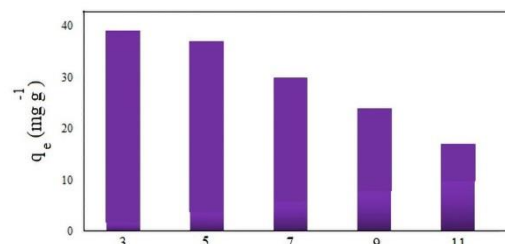


Fig. 8. Effect of pH on the removal efficiency of methyl orange by Fe₃O₄/polyaniline nanocomposite.

1.3. Adsorption isotherms

Appropriate correlations in the equilibrium considerations are known as a fundamental principle in the design of an adsorption system for removing pollutants. The adsorption isotherms describe how the adsorbed compounds interact with the adsorbent providing a comprehensive understanding of the nature of the adsorption procedure [36]. The adsorption isotherms imply the relationship between the quantity of adsorbed molecules at the constant temperature and equilibrium concentration in the solution. As a single operation, physico-chemical adsorption trend was also detected by obtained data from these isotherm models to investigate the applicability of the adsorption procedure [37]. To find information about the absorption trend, the data were fitted to three Langmuir, Freundlich and Dubinin-Radushkevich isotherm models.

Langmuir isotherm model. Langmuir theory was based on the assumption that the uptake of adsorbate takes place on a homogeneous surface via monolayer adsorption and adsorption energy is constant in this model. The Langmuir isotherm theory can be represented via the following equations:

$$\frac{1}{q_e} = \left(\frac{1}{K_L q_m} \right) \frac{1}{C_e} + \frac{1}{q_m} \quad (5)$$

where C_e (mg L⁻¹) is the equilibrium concentration of pollutant, q_e (mg g⁻¹) is the quantity of pollutant adsorbed at equilibrium, q_m (mg g⁻¹) is the maximum adsorption at monolayer and K_L (L mg⁻¹) is the Langmuir constant including the affinity of binding sites. The quantities of Langmuir factors can be determined from the slope and intercept of linear plots of $1/q_e$ against $1/C_e$.

Freundlich isotherm model.

The Freundlich isotherm model equation deals with physicochemical adsorption on heterogeneous surface at sites with various energy of adsorption and with non-identical adsorption sites that are not always available [38].

Freundlich theory is describe by the equation (6):

$$\ln q_e = \frac{1}{n} \ln C_e + \ln K_F \quad (6)$$

where K_F [(mg g⁻¹) (L mg⁻¹)^{1/n}] is the Freundlich constant and n is the heterogeneity parameter.

The K_F quantity is attributed to the adsorption capacity, while $1/n$ value is attributed to the adsorption intensity. K_F and $1/n$ are estimated from the linear plot of $\ln q_e$ versus $\ln C_e$. The K_F and n quantities are listed in Table 1.

Dubinin-Radushkevich (D-R) isotherm model. Dubinin-Radushkevich (D-R) isotherm is generally used to describe the sorption isotherms of a single solute system (Figure 9(c)). The D-R isotherm can also help to confirm that the adsorption process was chemisorption or physical adsorption [39].

D-R isotherm model can be expressed by equation (7):

$$\ln q_e = \ln q_m - K\varepsilon^2 \quad (7)$$

where q_e is equilibrium adsorbent-phase concentration of adsorbate (mg g⁻¹), and q_m is theoretical saturation capacity (mg g⁻¹). The plots of ε^2 vs. $\ln q_e$ were shown in Figure 9(c), and the values of K and $\ln q_m$ are estimated from the slope and intercept of the plots, respectively. K is the adsorption energy (mol² J⁻²), and ε is the polanyi potential (J mol⁻¹) which can be calculated through Eq. (8):

$$\varepsilon = RT \ln \left(1 + \frac{1}{C_e} \right) \quad (8)$$

where R is the universal gas constant (8.314 J mol⁻¹.K⁻¹), T is the Kelvin temperature (K), and C_e is the equilibrium aqueous phase concentration of adsorbate (mg L⁻¹).

The D-R model is mainly used to estimate the average free energy of adsorption (kJ mol⁻¹), as presented in equation (9):

$$E = \frac{1}{(-2R^{0.5})} \quad (9)$$

The magnitude of E can be applied to detect the mechanism of the adsorption procedure. For instance, when $E > 8$ kJ mol⁻¹, the adsorption procedure is chemical in nature.

Alternatively, when $E < 8$ kJ mol⁻¹, adsorption occurs through a physical procedure [40].

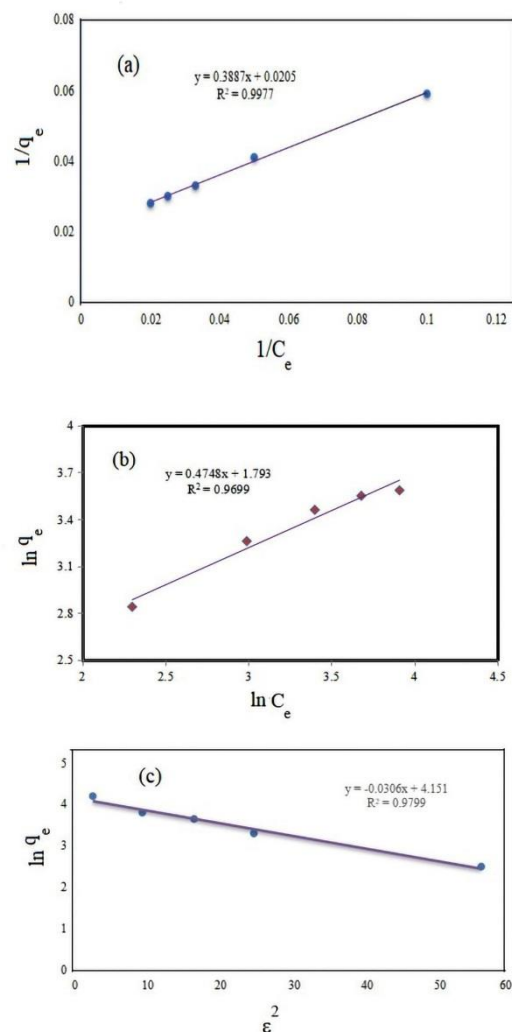


Fig. 9. Adsorption isotherms of methyl orange on Fe₃O₄/polyaniline composites with (a) Langmuir isotherm model, (b) Freundlich isotherm model, and (c) -Dubinin-Radushkevich isotherm model .

According to the Fig 9 and correlation coefficient quantities showed in Table 1, it can be seen that in all three Langmuir ($R^2 = 0.997$), Freundlich ($R^2 = 0.969$) and Dubinin Radushkevich models ($R^2 = 0.986$) the obtained R^2 quantities logically explain the goodness of fitting trend. According to these findings, in Langmuir model the adsorption procedure occurred uniformly and on a homogeneous surface as an adsorption monolayer without adsorbed molecules interaction. The K_1 factor (L mg⁻¹) is the equilibrium constant which related to the bond formation energy of the adsorption procedure, which implies the adsorption desirability, and its quantity was 0.052 for methyl orange implying a relatively strong bond with the adsorbent surface. According to Freundlich isotherm, the multilayer adsorption occurs with a non-uniform energy distribution of the adsorption sites as well as with the interference of adsorbed ions [41]. The factors of K_f and n are

the constants of Freundlich isotherm which reflect the absorption capacity and intensity, respectively [42]. Values of $1/n$ between 0 and 1 indicate the heterogeneity of the adsorbent. Obtained K_f value was $6.007 \text{ (mg g}^{-1}) \text{ (L mg}^{-1})^{1/n}$ for methyl orange and 0.474 for $1/n$, implying that the adsorption capacity and heterogeneity of the adsorbent are favorable. The Dubinin-Radushkevich model generally refers to the expression of the adsorption mechanism via the Gaussian energy distribution on a heterogeneous surface. Where parameter E (kJ mol^{-1}) represents the average absorption energy indicating the type of adsorption. For the adsorption of methyl orange on $\text{Fe}_3\text{O}_4/\text{polyaniline}$ nanocomposite, the value of E was obtained $3.651 \text{ kJ mol}^{-1}$, implying the adsorption of methyl orange on $\text{Fe}_3\text{O}_4/\text{polyaniline}$ nanocomposite occurs physically.

Table 1. Calculated various isotherm factors via linear method.

Type of isotherm model	Value
Langmuir isotherm	
$q_m \text{ (mg g}^{-1})$	48.78
$K_L \text{ (L mg}^{-1})$	0.052
R^2	0.997
Freundlich isotherm	
$K_F \text{ (mg g}^{-1}) \text{ (L mg}^{-1})^{1/n}$	6.007
n	2.1
R^2	0.969
Dubinin-Radushkevich (D-R) isotherm	
$K \text{ (mol}^2 \text{ J}^{-2})$	0.0375
$q_m \text{ (mg g}^{-1})$	8.08
$E \text{ (kJ mol}^{-1})$	3.651
R^2	0.986

1.4. Kinetics of adsorption

In order to characterize the kinetic behaviour of the procedure of methyl orange adsorption on $\text{Fe}_3\text{O}_4/\text{polyaniline}$ composite and assess the mechanism of the adsorption, two kinetic models of pseudo-first-order and pseudo-second-order, as the most widely applied models, were used.

Pseudo-first-order

The pseudo-first-order rate expression as a simple kinetic analysis can describe the kinetics of the adsorption process as follows Eq. (10) [43]:

$$\frac{dq_t}{dt} = k_{1,ads}(q_e - q_t) \quad (10)$$

where q_e , q_t (mg g^{-1}) and $k_{1,ads}$ (min^{-1}) are the amount of adsorbed dye at equilibrium and time t and the rate constant, respectively. After definite integration via using the initial conditions $q_t = 0$ at $t = 0$ and $q_t = q_t$ at $t = t$, Eq. (11) becomes:

$$\ln(q_e - q_t) = \ln q_e - k_{1,ads}t \quad (11)$$

The values of the pseudo-first order kinetic parameters were detected from the slope and intercept of linear plots of $\ln(q_e - q_t)$ against t . The results are summarized in Table 2.

Pseudo-second-order

The pseudo-second-order equation is based on adsorption equilibrium capacity and can be expressed (12) and presented linearly via the following Eq. (13)

$$\frac{dq_t}{dt} = k_{2,ads}(q_e - q_t)^2 \quad (12)$$

$$\frac{t}{q_t} = \frac{1}{k_{2,ads}q_e^2} + \left(\frac{1}{q_e}\right)t \quad (13)$$

where $k_{2,ads}$ ($\text{g mg}^{-1} \text{ min}^{-1}$) is the rate constant of the equation [44]. The quantities of the pseudo-second order kinetic factors were estimated from the slope and intercept of linear plots of t/q_t against t (The figures are not shown). From the slopes and intercepts, the values of q_e and $k_{2,ads}$ were calculated and summarized in Table 2.

The correlation coefficient (R^2) for both of kinetics models are presented in Table 2. The correlation coefficient of pseudo-second-order is greater than pseudo-first-order. Based on results, the adsorption kinetic of methyl orange on $\text{Fe}_3\text{O}_4/\text{polyaniline}$ fitted via pseudo-second-order.

Table 2. Kinetic parameters for methyl orange adsorption onto $\text{Fe}_3\text{O}_4/\text{polyaniline}$ nanocomposite.

Type of kinetic model	Value
Pseudo-first order model	
$q_e \text{ (mg g}^{-1})$	27.6
$k_{1,ads} \text{ (min}^{-1})$	0.11
R^2	0.975
Pseudo-second order model	
$q_e \text{ (mg g}^{-1})$	34.92
$k_{2,ads} \text{ (g mg}^{-1} \text{ min}^{-1})$	0.163
R^2	0.996

3.5. Thermodynamic study

Temperature can affect physical and chemical reactions. In order to investigate the influence of temperature on the adsorption of methyl orange by $\text{Fe}_3\text{O}_4/\text{polyaniline}$ nanocomposite, thermodynamic investigations were carried out at adsorbent dosage of 450 mg L^{-1} , pH 3, initial dye concentration of 20 mg L^{-1} and four different temperatures of 25, 30, 45 and $40 \text{ }^\circ\text{C}$. The Gibbs free energy changes (ΔG°) were determined using following Eq. (14):

$$\Delta G^\circ = -RT \ln K \quad (14)$$

where R , T (K) and K (q_e/C_e) are the universal gas constant, absolute temperature and the partition ratio, respectively [45]. The quantity of K and ΔG° are shown in Table 3. Standard enthalpy (ΔH°) and entropy (ΔS°) were detected by the Van't Hoff equation as follows Eq. (15) [45]:

$$\ln K = \left(\frac{\Delta S^\circ}{R}\right) - \left(\frac{\Delta H^\circ}{RT}\right) \quad (15)$$

ΔH° and ΔS° were obtained from the slope and intercept of the plot of $\ln k$ versus $1/T$, as presented in Fig. 10. The values of ΔH° and ΔS° are summarized in Table 3. Under constant reaction conditions, Gibbs free energy (ΔG°) varied from -

1.41 to $-1.69 \text{ kJ mol}^{-1}$, and the resulting ΔH° and ΔS° quantities were obtained 4.07 kJ mol^{-1} and $0.018 \text{ kJ mol}^{-1} \text{ K}^{-1}$, respectively.

The negative quantities of ΔG° indicate that the adsorption of methyl orange on $\text{Fe}_3\text{O}_4/\text{polyaniline}$ is spontaneous and thermodynamically favorable under the experimental conditions.

Positive values of ΔH° as well as the increasing trend of K with increasing temperature indicate that the adsorption of methyl orange on the surface of $\text{Fe}_3\text{O}_4/\text{polyaniline}$ nanocomposite is endothermic. The removal efficiency of methyl orange enhances with the enhancement in solution temperature.

When the temperature of the solution is increased, the pollutant molecules can move faster in the solution and the pollutant molecules mobility can be increased.

So, a number of molecules obtain enough energy to undergo an enhancing interaction with active sites at adsorbent surface.

From these results it was observed that adsorption of methyl orange by $\text{Fe}_3\text{O}_4/\text{polyaniline}$ nanocomposite is endothermic.

In endothermic reactions, if the temperature is enhanced, the amount of $T\Delta S^\circ$ (favorable parameter) also is enhanced and $T\Delta S^\circ$ acts as a favorable reaction agent.

On the other hand, as the temperature enhances, the adsorption rate also enhances [46]. This increased temperature can provide the energy needed for dehydration of pollutant molecules and the breakage of hydrogen bonds between the water molecules and the adsorbent surface leading to enhance in surface active sites [47].

Table 3. Thermodynamic factors (ΔH° , ΔG° , ΔS°) for the adsorption of methyl orange on $\text{Fe}_3\text{O}_4/\text{polyaniline}$ nanocomposite.

Temperature (K)	(ΔG°) (kJ mol ⁻¹)	(ΔS°) (kJ mol ⁻¹ K ⁻¹)	(ΔH°) (kJ mol ⁻¹)
298	-1.41	0.018	4.07
303	-1.49	-	-
308	-1.58	-	-
313	-1.69	-	-

3.6. Mechanism of Adsorption

With all the results above, the adsorption and desorption mechanism of methyl orange on $\text{Fe}_3\text{O}_4/\text{polyaniline}$ are described as below:

In solution, methyl orange molecule is dissociated into M-SO_3^- with M is an organic part of dyeing molecule. Polyaniline is backbone that will interact with M-SO_3^- . The electrostatic interactions are preferably involved in methyl orange adsorption onto polyaniline particles. In fact, at acidic pH, the adsorbent surface may be more positively charged (due to H^+ ions) which increases the electrostatic scattering between the dye anions and the adsorbent surface [48].

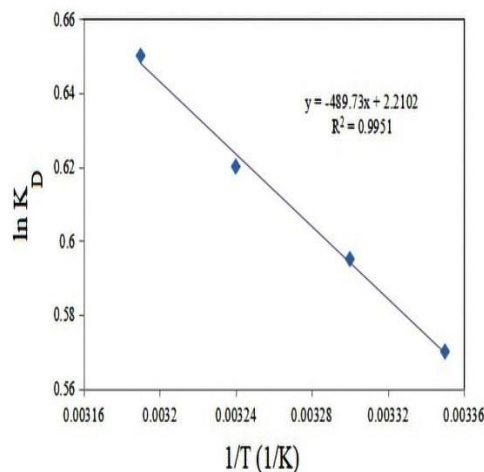


Fig. 10. Thermodynamic profile for adsorption of methyl orange on $\text{Fe}_3\text{O}_4/\text{polyaniline}$ nanocomposite.

Also, in acidic environments, the amino groups of polyaniline ($-\text{NH}_2$) are protonated in the presence of the released H^+ Protons in the environment; therefore, the adsorption of methyl orange, which has a negative charge, increases.

With protonation of the adsorption surface, the tendency of methyl orange to the adsorption surface increases. With the placement of polymer nanoparticles of polyaniline on the composite, more amino groups of polyaniline were available. Thus, more dye was adsorbed on the composite [31].

4. CONCLUSION

Fe_3O_4 , $\text{Fe}_3\text{O}_4/\text{polystyrene}$ and $\text{Fe}_3\text{O}_4/\text{polyaniline}$ were synthesized and employed as adsorbents for the removal of methyl orange from aqueous solutions. The results of the FT-IR, XRD, SEM, and VSM analyses showed that the synthesis of samples was carried out successfully.

It is concluded that $\text{Fe}_3\text{O}_4/\text{polyaniline}$ nanocomposite is more effective in the comparison with Fe_3O_4 , and $\text{Fe}_3\text{O}_4/\text{polystyrene}$ adsorbents. The results showed that all applied isotherm models logically described the adsorption process. The maximum methyl orange adsorption capacity was predicted as 48.78 mg g^{-1} via Langmuir model. Adsorption kinetics showed that pseudo second-order kinetic model was fitted logically to the experimental data.

Based on the results obtained from thermodynamic factors, it was concluded that the adsorption procedure was endothermic, feasible and spontaneous.

Acknowledgment

The authors acknowledge the support of Payame Noor University of Iran.

REFERENCES

- [1] G. K. Sarma, S. Sen Gupta, and K. G. Bhattacharyya, Nanomaterials as versatile adsorbents for heavy metal ions in water: a review, *Environ. Sci. Pollut. Res.* 26 (2019) 6245–6278.
- [2] S. Parlayici, Alginate-coated perlite beads for the efficient removal of methylene blue, malachite green, and methyl violet from aqueous solutions: kinetic, thermodynamic, and equilibrium studies, *Parlayici J. Anal. Sci. Technol.* 10 (2019) 1–15. using Fenton process, *J. Hazar. Mater.*, 294 (2015) 128–136.
- [3] R. Rahmawati, A. Taufiq, S. Sunaryono, A. Fuad, B. Yulianto, S. Suyatman, and D. Kurniadi, Synthesis of Magnetite (Fe₃O₄) Nanoparticles from Iron sands by Co-precipitation-Ultrasonic Irradiation Methods, *J. Mater. Environ. Sci.* 9 (2018) 155-160.
- [4] R. Xu, J. Mao, N. Peng, X. Luo, and C. Chang, Chitin/clay microspheres with hierarchical architecture for highly efficient removal of organic dyes, *Carbohydr Polym.* 188 (2018) 143–50.
- [5] X. Hou, G. Zhan, X. Huang, N. Wang, Z. Ai, and L. Zhang, Persulfate activation induced by ascorbic acid for efficient organic pollutants oxidation, *Chem. Eng. J.* 382 (2020) 122355-122362.
- [6] Y. Xu, Y. Wang, J. Wan, and Y. Ma, Reduced graphene oxide-supported metal organic framework as a synergistic catalyst for enhanced performance on persulfate induced degradation of trichlorophenol, *Chemosphere.* 240(2020) 124849-124857.
- [7] N. Ansari, and Z. Payami, Synthesis of Magnetic Graphene/Fe₃O₄ Nanocomposite by Electrochemical Exfoliation Method, *J. Nanostruct.* 10 (2020) 39-43.
- [8] M. Zirak, A. Abdollahiyan, B. Eftekhari-Sis, and M. Saraei, Carboxymethyl cellulose coated Fe₃O₄@SiO₂ core-shell magnetic nanoparticles for methylene blue removal: equilibrium, kinetic, and thermodynamic studies, *Cellulos* 25 (2017) 503-515.
- [9] M. M. Ayad, A. A. El-Nasr, and J. Stejskal, Kinetics and isotherm studies of methylene blue adsorption onto polyaniline nanotubes base/silica composite, *J. Ind. Eng. Chem.* 18 (2012) 1964–19699.
- [10] V. Sharma, P. Rekha, and P. Mohanty, Nanoporous hypercrosslinked polyaniline: an efficient adsorbent for the adsorptive removal of cationic and anionic dyes, *J. Mol. Liq.* 222 (2016) 1091–100.
- [11] A. N. Chishti, L. Ni, F. Guo, X. Lin, Y. i. Liu, H. Wu, M. Chen, and G. W. Diao, Magnetite-Silica core-shell nanocomposites decorated with silver nanoparticles for enhanced catalytic reduction of 4-nitrophenol and degradation of methylene blue dye in the water, *J. Environ. Chem. Eng.* 9 (2021) 104948-104455.
- [12] H. Pei, H. Zhang, Z. Mo, R. Guo, N. Liu, and Q. Jia, Highly efficient photocatalytic degradation of rhodamine B by conical graphene quantum dots/cerium oxide composite, *Cer. Int.* 46 (2020) 3827-3836.
- [13] Ziaadini, F. Mostafavi, A. Shamspur, T. Fathirad, Photocatalytic degradation of methylene blue from aqueous solution using Fe₃O₄@SiO₂@CeO₂ core-shell magnetic nanostructure as an effective catalyst, *Adv. Environ. Technol.* 2 (2019) 127-132.
- [14] R. Monsef, M. Ghiyasiyan-Arani, O. Amiri, M. Salavati Niasari, Sonochemical synthesis, characterization and application of PrVO₄ nanostructures as an effective photocatalyst for discoloration of organic dye contaminants in wastewater, *Ultrason. Sonochem.* 61 (2020) 104822-104829.
- [15] R. Monsef, M. Ghiyasiyan-Arani, M. Salavati Niasari, Design of Magnetically Recyclable Ternary Fe₂O₃/EuVO₄/g-C₃N₄ Nanocomposites for Photocatalytic and Electrochemical Hydrogen Storage, *ACS Appl. Energy Mater.* 4 (2021) 680–695.
- [16] S. Abdalkareem Jasima, M. M. Kadhim, B. Abed Hussein, S. Emad Izzate, and Z. Mohsen Najmf, Photocatalytic Degradation of Rhodamine B and Methylene blue Using α -Fe₂O₃ Nanoparticles, *Phys. Chem. Res.* 11 (2023), 139-147.
- [17] T. Tran, H. Duong, T. Pham, T. Nguyen, T. Nguyen, and B. Tran, Preparation of Magnetic Composite Polyaniline/Fe₃O₄-Hydrotalcite and Performance in Removal of Methyl Orange, *Adsorp, Sci. Tech.* (2021), 18 pages.
- [18] R. Mohammadi, B. Massoumi, and R. Mashayekhi, Fe₃O₄/polystyrene-alginate nanocomposite as a novel adsorbent for highly efficient removal of dyes, *J. Chem. Chem. Eng.* 41 (2022) 3553-3566.
- [19] M. Ghanbari, M. Salavati-Niasari, Ti₄CdI₆ nanostructures: facile sonochemical synthesis and photocatalytic activity for removal of organic dyes, *Inorganic Chem.* 57 (2018) 11443–11455.
- [20] S. B. Hammouda, N. Adhoum, and L. Monser, Synthesis of magnetic alginate beads based on Fe₃O₄ nanoparticles for the removal of 3-methylindole from aqueous solution, *J. Hazard. Mater.* 294 (2015) 128-136.
- [21] H. A. Tayebi, Z. Dalirandeh, A. Shokuhi Rad, A. Mirabi, and E. Binaeian, Synthesis of polyaniline/Fe₃O₄ magnetic nanoparticles for removal of reactive red 198 from textile waste water: kinetic, isotherm, and thermodynamic studies, *Desal. Wat. Treat.* 57 (2016) 22551-22563.
- [22] F. Seifikar, and S. Azizian, A facile method for precipitating of dispersed carbon particles prepared by microwave heating and its application for dye removal, *J. Mol. Liq.* 275 (2019) 394–401.

- [23] S. Kocaoba, Adsorption of Fe(II) and Fe(III) from aqueous solution by using sepiolite: Speciation studies with MINEQL+ computer program, *Sep. Sci. Technol.* 55 (2020) 896–906 .
- [24] R. Mohammadi, B. Massoumi, and F. Galandar, Polyaniline-TiO₂ /graphene nanocomposite: an efficient catalyst for the removal of anionic dyes, *Desal. Wat. Treat.* 142 (2019) 321–330.
- [25] M. N. Pervez, W. He, T. Zarra, V. Naddeo, and Y. Zhao, New Sustainable Approach for the Production of Fe₃O₄/Graphene Oxide-Activated Persulfate System for Dye Removal in Real Wastewater, *Water* 12 (2020) 733-750.
- [26] N. Shirzad Taghanaki, N. Keramati, and M. Mehdipour, Photocatalytic Degradation of Ethylbenzene by Nano Photocatalyst in Aerogel form Based on Titania, *J. Chem. Chem. Eng.* 40 (2021) 525-537 .
- [27] P. Toktam, Z. Es'haghi, A. Ahmadvour, and A. Nakhaei, Optimization of Adsorption Parameters Using Central Composite Design for the Removal of Organosulfur in Diesel Fuel by Bentonite-Supported Nanoscale NiO-WO₃, *J. Chem. Chem. Eng.* 41 (2022) 808-820 .
- [28] Y. Wang, L. Gai, W. Ma, H. Jiang, X. Peng, and L. Zhao, Ultrasound-Assisted Catalytic Degradation of Methyl Orange with Fe₃O₄/Polyaniline in Near Neutral Solution, *Ind. Eng. Chem. Res.* 54 (2015) 2279–2289.
- [29] B.D. Deshpande, P.S. Agrawal, M.K.N. Yenkie, and J.S. Dhoble, Prospective of Nanotechnology in Degradation of Waste Water: A New Challenges, *Nano-Struct. Nano-Objects.* 22 (2020) 100442.
- [30] M. A. Ebrahimzadeh, A. Naghizadeh, O. Amiri, M. Shirzadi-Ahodashia, and S. Mortazavi-Derazkola, Green and Facile Synthesis of Ag Nanoparticles Using Crataegus Pentagyna Fruit Extract (CP-AgNPs) for Organic Pollution Dyes Degradation and Antibacterial Application, *Bioorg. Chem.* 94 (2020) 103425-103433.
- [31] M. Jokar, R. Foroutani, M. H. Safaralizadeh, and K. Farhadi, Synthesis and Characterization of Polyaniline/Fe₃O₄ Magnetic Nanocomposite as Practical Approach for Fluoride Removal Process, *Annu. Res. Rev. Bio.* 4 (2014) 3262-3273.
- [32] E. A. Abdelrahman, D. A. Tolan, and M.Y. Nassar, A tunable template-assisted hydrothermal synthesis of hydroxysodalite zeolite nanoparticles using various aliphatic organic acids for the removal of zinc (II) ions from aqueous media, *J. Inorg. Organomet. Polym.Mater.* 29 (2019) 229–247.
- [33] E. Parthiban, N. Kalavivasan, and S. Sudarsan, A study of magnetic, antibacterial and antifungal behaviour of a novel gold anchor of polyaniline/itaconic acid/Fe₃O₄ hybrid nanocomposite: Synthesis and characterization, *Arabian. J. Chem.* 13 (2020) 4751–4763.
- [33] M. M. Ayad, W. A. Amer, M. G. Kotp, I. M. Minisy, A. F. Rehab, D. S. Kopecky, and P. Fitl, Synthesis of silver-anchored polyaniline–chitosan magnetic nanocomposite: a smart system for catalysis, *RSC Adv.* 7 (2017) 18553.
- [35] M. R. Patil., S. D. Khairnar, and V. S. Shrivastava, Synthesis, characterisation of polyaniline–Fe₃O₄ magnetic nanocomposite and its application for removal of an acid violet 19 dye, *Appl. Nanosci.* 6 (2016) 495–502.
- [36] S. Mnasri Ghnimi, and N. Frini-Srasra, A comparison of single and mixed pillared clays for zinc and chromium cations removal, *Appl. Clay Sci.* 158 (2018) 150–157.
- [37] Xia, X. Liu, Z. Chen, L. Fang, H. Du, and X. Zhang, Efficient and sustainable treatment of anionic dye wastewaters using porous cationic diatomite, *J. Taiwan. Inst. Chem. Eng.* 113 (2020) 8–15.
- [38] X. Yan, Q. He, X. Zhang, H. Gu, H. Chen, Q. Wang, L. Sun, Wei, and S. Z. Guo, Magnetic Polystyrene Nanocomposites Reinforced with Magnetite Nanoparticles, *Macromol. Mater.Eng.* 299 (2014) 485–494.
- [39] Y. H. Zhao, J.T. Geng, J. C. Cai, Y. F. Cai, and C.Y. Cao, Adsorption performance of basic fuchsin on alkali-activated diatomite, *Adsorpt. Sci. Technol.* 38 (2020) 151–167.
- [40] E. A. Abdelrahman, and R. M. Hegazey, Utilization of waste aluminum cans in the fabrication of hydroxysodalite nanoparticles and their chitosan biopolymer composites for the removal of Ni (II) and Pb (II) ions from aqueous solutions: kinetic, equilibrium, and reusability studies, *Microchem J.* 145 (2019) 18–25.
- [41] A. Oussalah , A. Boukerroui , A. Aichour , and B. Djellouli, Cationic and anionic dyes removal by low-cost hybrid alginate/natural bentonite composite beads: adsorption and reusability studies, *Int. J. Biol. Macromol.* 124 (2019) 854–862.
- [42] S. C. Azimi, and S. Farhad, Advanced Oxidation Process as a Green Technology for Dyes Removal from Wastewater: A Review, *Iran. J. Chem. Chem. Eng.* 40 (2021) 1467-1489.
- [43] D. B. Jiang , X. Liu , X. Xu, and Y. X. Zhang , Double-shell Fe₂O₃ Hollow Box-Like Structure for Enhanced Photo-Fenton Degradation of Malachite Green Dye, *J. Phys. Chem. Solids.* 112 (2018) 209-215 .
- [44] A. Naghizadeh, and M. Ghafouri, Synthesis and Performance Evaluation of Chitosan Prepared from Persian Gulf Shrimp Shell In Removal of Reactive Blue 29 Dye from Aqueous Solution (Isotherm, thermodynamic and kinetic study), *Iran. J. Chem. Chem. Eng.* 36 (2017) 25-36 .
- [45] Zhu, F. Liu, C. Ling, H. Jiang, H. Wu, and A. Li, Growth of graphene-supported hollow cobalt sulfide nanocrystals via MOF-templated ligand

- exchange as surface-bound radical sinks for highly efficient bisphenol A degradation, *Appl. Catal. B-Environ.* 242 (2019) 238–248.
- [46] Z. Dong, Q. Zhang, B. Y. Chen, and J. Hong, Oxidation of bisphenol A by persulfate via Fe₃O₄- α -MnO₂ nanoflower-like catalyst: Mechanism and efficiency, *Chem. Eng. J.* 357 (2019) 337–347.
- [47] H. Jafari, G. R. Mahdavinia, B. Kazemi Heragh, S. Javanshir, and S. Alinavaz, Basic Dyes Removal by Adsorption Process Using Magnetic Fucus Vesiculosus (Brown Algae), *J. Wat. Environ. Nanotechnol.* 5 (2020) 256-269.
- [48] M. Soleymani, A. Akbari, and G. R. Mahdavinia, Magnetic PVA/ laponite RD hydrogel nanocomposites for adsorption of model protein BSA, *Polym. Bulletin.* 76 (2018) 2321- 2340.



COPYRIGHTS

© 2022 by the authors. Licensee PNU, Tehran, Iran. This article is an open access article distributed under the terms and conditions of the Creative Commons Attribution 4.0 International (CC BY4.0) (<http://creativecommons.org/licenses/by/4.0>)

مقایسه میزان توانایی نانوکامپوزیتهای مغناطیسی اکسید آهن، اکسید آهن / پلی استایرن و اکسید آهن / پلی آنیلین در حذف متیل اورانژ از محلولهای آبی

رباب محمدی^{۱*}، بخشعلی معصومی، امین مشایخی

بخش شیمی، دانشگاه پیام نور، تهران، ایران

* E-mail: rb_mohammadi@pnu.ac.ir; mohammadi_rb@yahoo.com

تاریخ دریافت: ۱۵ مرداد ۱۴۰۲ تاریخ پذیرش: ۱۹ شهریور ۱۴۰۲

چکیده

در این تحقیق، نانوترکیبات اکسید آهن، اکسید آهن / پلی استایرن و اکسید آهن / پلی آنیلین تهیه و در جذب سطحی متیل اورانژ از محلولهای آبی مورد مقایسه قرار گرفتند. مورد مطالعه قرار گرفت FT-IR. استفاده از ساختار شیمیایی ترکیبات تهیه شده با فاز کریستالی اکسید آهن، اکسید آهن / پلی استایرن و اکسید آهن / پلی آنیلین با استفاده از XRD مورد شناسایی قرار گرفت. برای تعیین مورفولوژی نمونه های سنتز شده از SEM استفاده گردید. خاصیت مغناطیسی نمونه های سنتز شده با موفقیت بررسی شد. نانوترکیبات سنتز شده در حذف متیل اورانژ از محلولهای آبی مورد استفاده قرار گرفتند. بر اساس نتایج به دست آمده، نانوکامپوزیت اکسید آهن / پلی آنیلین کارایی بالاتری را در حذف متیل اورانژ نشان داد که دلیل آن، بار مخالف متیل اورانژ و نانوکامپوزیت اکسید آهن / پلی آنیلین است. متغیرهای موثر در حذف متیل اورانژ نظیر مقدار جاذب، و زمان تماس بررسی و بهینه سازی شدند. مقادیر بهینه برای مقدار جاذب، و زمان تماس به ترتیب ۳-۴، ۴۵۰ میلی گرم بر لیتر و ۵۰ دقیقه به دست آمد. برای تعیین نوع ایزوترم جذب، ایزوترم های لانگمیر، فروندلیچ و دوبینین رادشکویچ مطالعه شدند. طبق ایزوترم لانگمیر، جاذب مغناطیسی اکسید آهن / پلی آنیلین بالاترین ظرفیت معادل ۴۷.۷۶ میلی گرم بر گرم را در جذب سطحی متیل اورانژ نشان داد. مطالعات سینتیکی نشان داد جذب سطحی متیل اورانژ با استفاده از مدل سینتیکی شبه درجه دوم قابل توجیه است. تحت شرایط کنترل شده واکنش، انرژی آزاد گیبس از ۱.۴۱- تا ۱.۶۹- کیلوژول بر مول تغییر کرد. همچنین برای تغییرات آنتالپی و تغییرات آنتروپی، به ترتیب مقادیر ۴۰.۷ کیلوژول بر مول و ۰.۱۸ کیلوژول بر مول بر کلون به دست آمد. از این رو میتوان نتیجه گرفت جذب سطحی متیل اورانژ بر روی جاذب اکسید آهن / پلی آنیلین، فرایندی خودبخودی و گرماگیر است.

کلید واژه ها

اکسید آهن / پلی استایرن، اکسید آهن / پلی آنیلین، حذف متیل اورانژ، ظرفیت جذب سطحی، مطالعات سینتیکی.